



OPEN

# miRNA-338-3p influences the liver cancer stem cells and lenvatinib resistance properties by targeting SOX4

Ying Yuan<sup>1,3</sup>, Hui-fen Li<sup>2,3</sup>✉, Zi-mei Liu<sup>1</sup>✉ & Li-ping Yu<sup>1</sup>✉

Cancer stem cells (CSCs) are critical players in the pathogenesis of human-associated cancers. It is well established that the stemness of CSCs is modulated by microRNA (miRNA). In the current study, the miR-338-3p deficiency increased self-renewal and tumor malignancy in hepatic CSCs. Nevertheless, miR-338-3p overexpression suppresses tumorigenesis and self-renewal in liver CSCs. Mechanistically, miR-338-3p specifically targets SOX4 in liver CSCs. Moreover, miR-338-3p-associated downregulation of SOX4 prevents tumorigenesis and self-renewal in the CSCs of the liver. The miR-338-3p overexpression in hepatocellular carcinoma (HCC) cells was responsive to lenvatinib-induced apoptosis and cell progression inhibition. Patients' cohort shows that miR-338-3p may predict Lenvatinib benefits in HCC patients. Furthermore, by decreasing the miR-338-3p overexpression sensitivity to Lenvatinib-induced cell death in HCC cells, SOX4 may be a potential therapeutic candidate. In conclusion, miR-338-3p has a considerable function in liver CSC self-renewal and tumor development, making it a promising therapeutic target against HCC.

**Keywords** Liver cancer stem cell, Hepatocellular carcinoma, miR-338-3p, SOX4, lenvatinib

## Abbreviations

CSCs	Cancer stem cells
HCC	Hepatocellular carcinoma
T-ICs	Tumor-initiating cells
NC	Negative control
PDX	Derive xenograft

The malignancy hepatocellular carcinoma (HCC) impacts the liver. It is the sixth-primary contributor of mortalities due to cancer globally and is the most common cancer with the highest incidence<sup>1</sup>. Surgical excision is the most effective method for early diagnosis of HCC<sup>2</sup>. Surgical excision and liver transplantation offer the only hope of a cure; however, both procedures have limited utility. Moreover, most HCC patients are detected at the middle to progressive stage<sup>3</sup>. Lenvatinib is the latest approved targeted drug for treating advanced HCC<sup>4</sup>. It has been reported to be more effective than sorafenib. Many people with HCC are resistant to Lenvatinib. The negative effects for some patients with HCC can be rather severe<sup>5,6</sup>. Finding biomarkers of Lenvatinib responsiveness and understanding the mechanism of Lenvatinib resistance is paramount.

CSCs, or cancer stem cells, are a subset of cancer cells and have an illimitable competence for proliferation and division<sup>7,8</sup>. CSCs have been linked to controlling tumor growth, spread, relapse, and resistance to chemotherapy<sup>9-11</sup>. CSCs are the decisive factors in tumor metastasis and recurrence<sup>12,13</sup>. The presence of hepatic CSCs has also been established by prior research<sup>14</sup>. However, the mechanism behind the spread of hepatic CSCs is still a mystery.

MicroRNAs (miRNAs) are non-coding RNA molecules that considerably contribute to gene regulation and are extremely tiny and highly conserved<sup>15</sup>. Multiple studies have demonstrated the significance of miRNAs in controlling several biological processes<sup>16</sup>. In certain malignancies, miRNAs function either as a tumor suppressor or an oncogene<sup>17-19</sup>. Improvements in therapeutics require a better knowledge of miRNA molecular

<sup>1</sup>Department of Oncology, Tongren Hospital, Shanghai Jiao Tong University School of Medicine, 1111, Xianxia Road, Shanghai 200336, China. <sup>2</sup>Department of Hepatic Surgery & Interventional Radiology, Eastern Hepatobiliary Surgery Hospital, Second Military Medical University, Shanghai, China. <sup>3</sup>Ying Yuan and Hui-fen Li contributed equally to this work. ✉email: huifen0823@163.com; lzm890819@163.com; atplx@163.com

pathways, which would shed light on the development and advancement of cancer and other disorders. Furthermore, multiple types of cancer, including HCC, have been linked to miR-338-3p's involvement in tumor progression<sup>20–22</sup>. The probable function of miR-338-3p in hepatic CSCs is undetermined. Our findings indicated that miR-338-3p was suppressed in hepatic CSCs.

In addition, the miR-338-3p selectively targeting SOX4 repressed the self-renewal and carcinogenesis of hepatic CSCs in vitro and in vivo. Moreover, miR-338-3p is critical in determining Lenvatinib's efficacy in HCC. As a result, miR-338-3p is a possible marker for the effectiveness of the drug Lenvatinib and an alternative therapy for HCC.

## Materials and methods

### HCC's sample collection

A total of 35 Specimens were acquired from individuals who had undergone primary HCC resection underwent adjuvant Lenvatinib therapy from 2018 to 2020 following primary HCC surgery. The tissues from 35 HCC patients were utilized to study the miR-338-3p correlation with SOX4. RT-PCR assay was utilized for the miR-338-3p and SOX4 expression levels evaluations.  $\beta$ -actin served as a reference for normalizing RT-PCR data, then subjecting it to Spearman's correlation analysis for further evaluation. All patients provided informed consent. In addition, the sampling procedures were conducted with authorization from the Tongren Hospital, Shanghai Jiao Tong University School of Medicine Ethical Committee review board. All methods were carried out in accordance with relevant guidelines and regulations for human studies. The characteristics of the patient cohort was listed in supplement Table 1.

### Cell culture

The culturing of HCC cell lines, including Hep3B and Huh7, was performed in DMEM enriched with FBS (10%), L-glutamine (2 mM), and gentamicin (25  $\mu$ g/ml) and were incubated with 5% CO<sub>2</sub> at 37 °C. The miR-338-3p knockdown lentivirus and their control lentivirus (China) were utilized to infect the underlined cell lines, followed by evaluating stable infections via puromycin. Huh7, Hep3B, and SNU398 cells were treated with Lenvatinib (Selleck, S1164) at a dosage level under their IC<sub>50</sub>, and then the dose was increased (0.2  $\mu$ M/L each week for 6 to 7 months) to generate Lenvatinib-resistant cell lines. Through prolonged culturing in the presence of Lenvatinib, three cell lines with acquired resistance were established and maintained.

### RNA interference

The siRNAs against NC siRNA and SOX4 were constructed by Ribobio (China). The target sequence of SOX4 siRNA is 5'-GGACAGACGAAGAGUUUAATT-3'. HCC cells were transfected with siRNAs at 200 nM through a siRNA transfection reagent (Polyplus, France). The transfection of HCC cells was carried out using SOX4 siRNA or an NC, and then spheroids were formed, followed by in vitro and in vivo LDA post miR-338-3p suppression.

### In vivo experiments

Each in vivo experiment was performed as recommended by the Animal Care and Use Committee of the the Tongren Hospital, Shanghai Jiao Tong University School of Medicine. NOD-SCID mice (age=4 to 6 weeks) were acquired from SIPP-BK Experimental Animal Co. China, kept in sterile environments, and fed a normal chow diet. HCC cells were diluted in sequence to the relevant concentrations ( $1 \times 10^3$ ,  $5 \times 10^3$ ,  $1 \times 10^4$ ,  $5 \times 10^4$ ) and combined with 100  $\mu$ l Matrigel gel (1:1) for in vivo limited dilution experiment followed by injecting the underlined cells subcutaneously into mice ( $n=6$ , randomized) and were slaughtered after eight weeks to count the number of tumors. The maximal tumor size was less than 2000 mm<sup>3</sup> permitted the the Animal Care and Use ethics committee of the Tongren Hospital, Shanghai Jiao Tong University School of Medicine. The maximal tumor size in all mice involved in this study was not exceeded than 2000 mm<sup>3</sup>. All mice were killed by dislocation of the cervical vertebrae. The study was carried out in compliance with the ARRIVE guidelines.

### In vitro spheroid formation assay

The DMEM/F12 medium (Gibco) supplemented with 20 ng/mL EGF, 1% FBS, and 20 ng/mL bFGF was used to culture HCC cells for one week at a 300 cells/well density on 96-well culture plates purchased from Corning Incorporated Life Sciences, USA. The spheroids were determined and displayed. The same findings were obtained in three individual experiments.

### Limiting Dilution assay (LDA)

For one week, cells were cultured in 96-well culture plates at 2, 4, 8, 16, 32, and 64 cell densities ( $n=8$ ) in DMEM/F12 medium containing 20 ng/mL of EGF, 20 ng/mL of bFGF, and 1% FBS.

The ELDA, a software application for LDA data analyses, assessed the CSC's abundance. Each experimental procedure was repeated three times, and the same findings were obtained in all three experiments.

### CTC isolation and flow-cytometric evaluations

To separate CD133 and CD90 positive cells, primary and HCC cells or tissues were exposed to anti-CD90 or primary anti-CD133 for 0.5 h at ~ 25 °C. Flow cytometry was then performed on the cells through a Beckman Coulter MoFlo XDP cell sorter (located in Indianapolis, Indiana, USA) following the supplier's guidelines. On the segregated cells from the 3 distinct analyses, RT-PCR was performed. Each experimental procedure was performed thrice.

### Apoptotic assay

Lenvatinib treatment (10  $\mu$ M) was provided to cells with elevated expression of miR-338-3p and their control HCC cells for 48 h. Then, staining was performed using 7-AAD and Annexin-V kit at  $\sim$  25 °C for 15 min without light. Following that, a flow cytometer was used to examine the cell apoptosis utilizing an Annexin V-FITC Apoptosis Detection Kit I from BD Pharmingen in San Diego, USA, per the manufacturer's recommendations. Each experimental procedure was conducted thrice.

### The luciferase assay

The conserved miR-338-3p-interacting regions from the SOX4 3'UTR, a 500-bp segment, were incorporated into a luciferase reporter plasmid. The putative miR-338-3p-interacting base sequence "UGCUGGA" was mutated to "GGGGGGGA" in the SOX4 3'UTR mutant luciferase plasmid. Next, it was introduced a 500-bp fragment of the SOX4 mutant 3'UTR. HCC cells were grown in 24-well plates with or without miR-338-3p and then co-transfected with the pRLCMV vector (2 ng/well, internal control, Promega), resulting in luciferase UTR-report vector (100 ng/well), and miR-338-3p precursor or control (20 ng/well, Applied Biosystems) through Lipofectamine 2000 (Invitrogen). The (DLR™) Assay (Promega) extended the relative luciferase activity after 24 h of cell lysis. Each experimental procedure was conducted thrice.

### Real-time PCR (RT-PCR)

TRIZOL-based total RNA extraction (from cells/tissues) was performed as suggested by the manufacturer. Agarose gel electrophoresis and a UV NanoDrop ND-1000 spectrophotometer were used to confirm RNA purity and integrity accordingly. The M-MLV RTase cDNA Synthesis Kit (Promega) synthesized cDNA from the recovered RNA via reverse transcriptase. Next, a LightCycler 480 System and SYBR Green PCR Kit from Roche were used to evaluate the RT-PCR assay. The PCR comprised a denaturation step (for 40 cycles of 15s at 95 °C), followed by annealing (for 30s at 60 °C), and the final extension (for 30s at 72 °C). Next, melting curves were used to validate primers specificity. Biological triplicates of each sample's measurements were taken. The sequences of primers used are as follows.

U6 primer sequences:

Forward: 5' ATTGGAACGATAACAGAGAAGATT 3'.

SOX4.

Reverse: 5' ACACGGCATATTGCACAGGA 3',

Forward: 5' GCACTAGGACGTCTGCCTT 3'.

$\beta$ -actin.

Reverse: 5' AATGGCACCCCTGCTCACGCA 3',

Forward: 5' GGCCCAGAATGCAGTCGCCTT 3'.

### Immunoblotting

As discussed earlier, cell lysis buffer was used to obtain samples<sup>23</sup>. SDS-PAGE was employed to isolate protein (25  $\mu$ g), then transferred to the NC membrane. Non-fat milk (5%) was utilized for the membrane blockage, followed by incubating with the primary antibody, and then incubation was conducted with a secondary antibody (conjugated with IRDye 800CW). The detection of fluorescence intensity was carried out with the LI-COR imaging system Biosciences, USA. The primary antibodies, including  $\beta$ -actin (1:1000; 27309-1-AP, Proteintech) and SOX4 (1:1000, ab86809, Abcam), were utilized in the underlined experiment.

### Statistical evaluations

All statistical analyses were conducted through the GraphPad Prism program. Each experimental procedure was performed in triplicate. The obtained data were indicated as the mean  $\pm$  s.d. Bonferroni Multiple Comparisons or t-test was employed for the statistical assessment. The statistical significance was deemed at a p-value of  $< 0.05$ .

## Results

### Reduced expression of miR-338-3p in hepatic CSCs

CD133 and CD90 have already been established as markers of liver CSCs<sup>24,25</sup>. Pearson correlation analysis showed an inverse relationship between the levels of miR-338-3p and the expressions of CD133 ( $R^2 = 0.608, P < 0.001$ ) and CD90 ( $R^2 = 0.4736, P < 0.001$ ) in tumor cells extracted from primary HCC tissues. This relationship can be observed in Fig. 1A and B, respectively. Next, flow cytometric evaluations were used to isolate and enhance liver CSCs by sphere formation. Isolated CD133 + or CD90 + HCC cells indicated decreased miR-338-3p levels relative to CD90- CD133-HCC cells (Fig. 1C and D), as predicted. The miR-338-3p expression was considerably lowered in HCC spheres relative to adherent HCC cells (Fig. 1E). Notably, as HCC spheroids were cultured for successively longer periods, expression of miR-338-3p was considerably lowered, as depicted in Fig. 1F.

### Attenuation of hepatic CSCs self-renewal, tumor formation by miR-338-3p

To investigate the potential role of miR-338-3p in hepatic CSCs, an overexpression virus for miR-338-3p was applied to infect Huh7 and Hep3B cells, and the results of this experiment were analyzed using RT-PCR (Fig. 2A). Relative to the control HCC cells, the cells with elevated expression of miR-338-3p displayed low

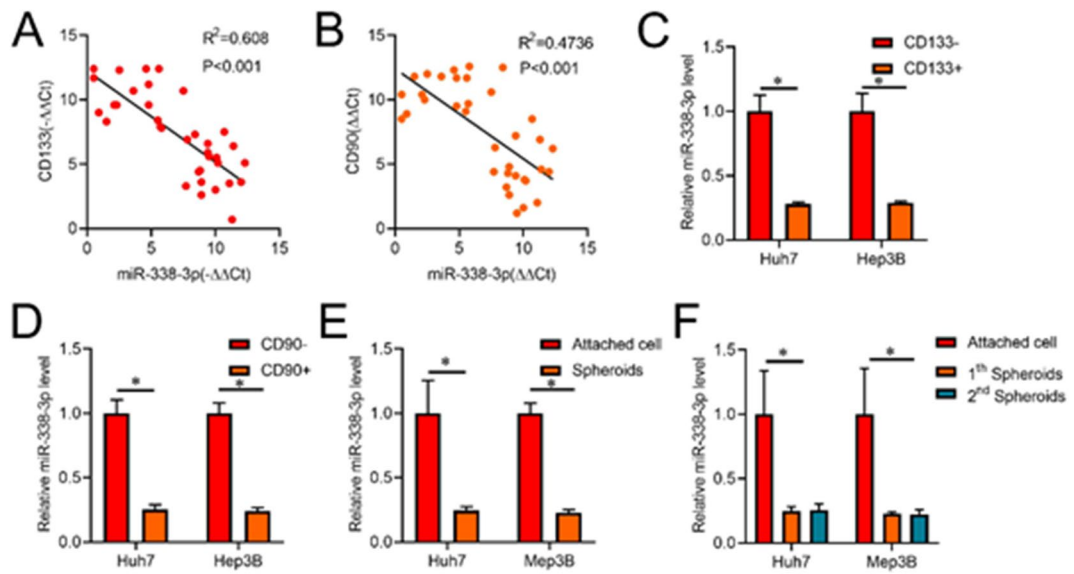


**Fig. 1.** Downregulation of miR-338-3p expression in hepatic CSCs. (A) Primary HCC cells ( $n=35$ ) were analyzed for their miR-338-3p and CD133 expression levels using RT-PCR. Spearman's correlation analysis was performed after data were standardized to  $\beta$ -actin as  $\Delta\Delta Ct$ . (B) Using RT-PCR, we analyzed the relationship between miR-338-3p expression and CD90 expression in primary HCC cells ( $n=35$ ). Spearman's correlation analysis was performed after data were standardized to  $\beta$ -actin as  $\Delta\Delta Ct$ . (C) We used RT-PCR to examine miR-338-3p expression in CD133+ and CD133- HCC cells, accordingly. (D) Using RT-PCR, we evaluated miR-338-3p expression between CD90+ HCC cells and CD90- HCC cells. (E) RT-PCR was utilized to examine miR-338-3p expression in HCC spheroids and adherent cells. (F) RT-PCR measured miR-338-3p expression in HCC spheroids collected in serial passages. Error bars shows mean  $\pm$  SD derived from  $n=3$  independent experiments,  $*p < 0.05$ .

CSCs markers (Fig. 2B and C). Moreover, miR-338-3p overexpressed cells exhibited impaired self-renewal capacity (Fig. 2D). In vitro, LDAs indicated the CSCs proportion in miR-338-3p overexpressed HCC cells was significantly decreased, as depicted in Fig. 2E. Moreover, in vivo, LDA showed that the tumorigenesis capacity was dramatically impaired by an elevated miR-338-3p expression in HCC (Fig. 2F). Next, the miR-338-3p suppression virus was used to infect Huh7 and Hep3B cells, then evaluating their impact via RT-PCR (Fig. 3A). The miR-338-3p knockdown cells showed increased CSCs markers than the control HCC cells (Fig. 3B and C). Moreover, miR-338-3p suppression cells exhibited enhanced self-renewal capacity (Fig. 3D). The ratio of CSCs in miR-338-3p suppression HCC cells was much higher, according to in vitro LDA (Fig. 3E). Furthermore, in vivo, LDA suggested that the tumorigenesis capacity was markedly enhanced through miR-338-3p knockdown in HCC (Fig. 3F). The outcomes indicated that miR-338-3p attenuates self-renewal, tumor formation in HCC.

### Suppression of SOX4 expression by miR-338-3p targeting its 3'-UTR

Subsequently, we employed TargetScan to anticipate possible direct targets of miR-338-3p and discovered that numerous genes have a potential miR-338-3p interacting site; among these was a gene called SOX4, which has been linked to CSC regulation<sup>26</sup>. Figure 4A and B indicates that when miR-338-3p was suppressed, SOX4 transcriptional and translational levels elevated. When SOX4 transcriptional and translational levels decreased in HCC with miR-338-3p Mimic (Figure S1A and B). The whole 3'-UTR of the SOX4 gene was isolated and cloned downstream of the Renilla luciferase gene to confirm that SOX4 is a direct target of miR-338-3p (Fig. 4C). Figure 4D shows that when the reporter construct included the wild-type 3'-UTR, miR-338-3p knockdown elevated luciferase activity. Moreover, the miR-338-3p-mediated elevation in luciferase activity was lost when the targeting site was mutated. Furthermore, miR-338-3p levels were negatively related to SOX4 expression in tumor cells isolated from primary HCC tissues using Pearson correlation analysis (Fig. 4E).

### Attenuation of hepatic CSCs self-renewal and tumor formation via targeting SOX4 by miR-338-3p

The particular SOX4 siRNA was transfected into HCC cells containing miR-338-3p knocked down and control cells to verify the functional link between SOX4 and miR-338-3p. Figure 4F shows that the variation in self-renewal capability between miR-338-3p knockdown and control HCC cells was attenuated by using a specific SOX4 siRNA. Next, using a particular SOX4 siRNA eliminated the gap between the control HCC cells and miR-338-3p knockdown in the percentage of CSCs (Fig. 4G). Specific SOX4 siRNA also eliminated the difference in tumorigenic potential between control HCC cells and miR-338-3p knockdown cells (Fig. 4H). The underlined data suggested that the expression of SOX4 was needed for miR-338-3p to develop CSCs in the liver.

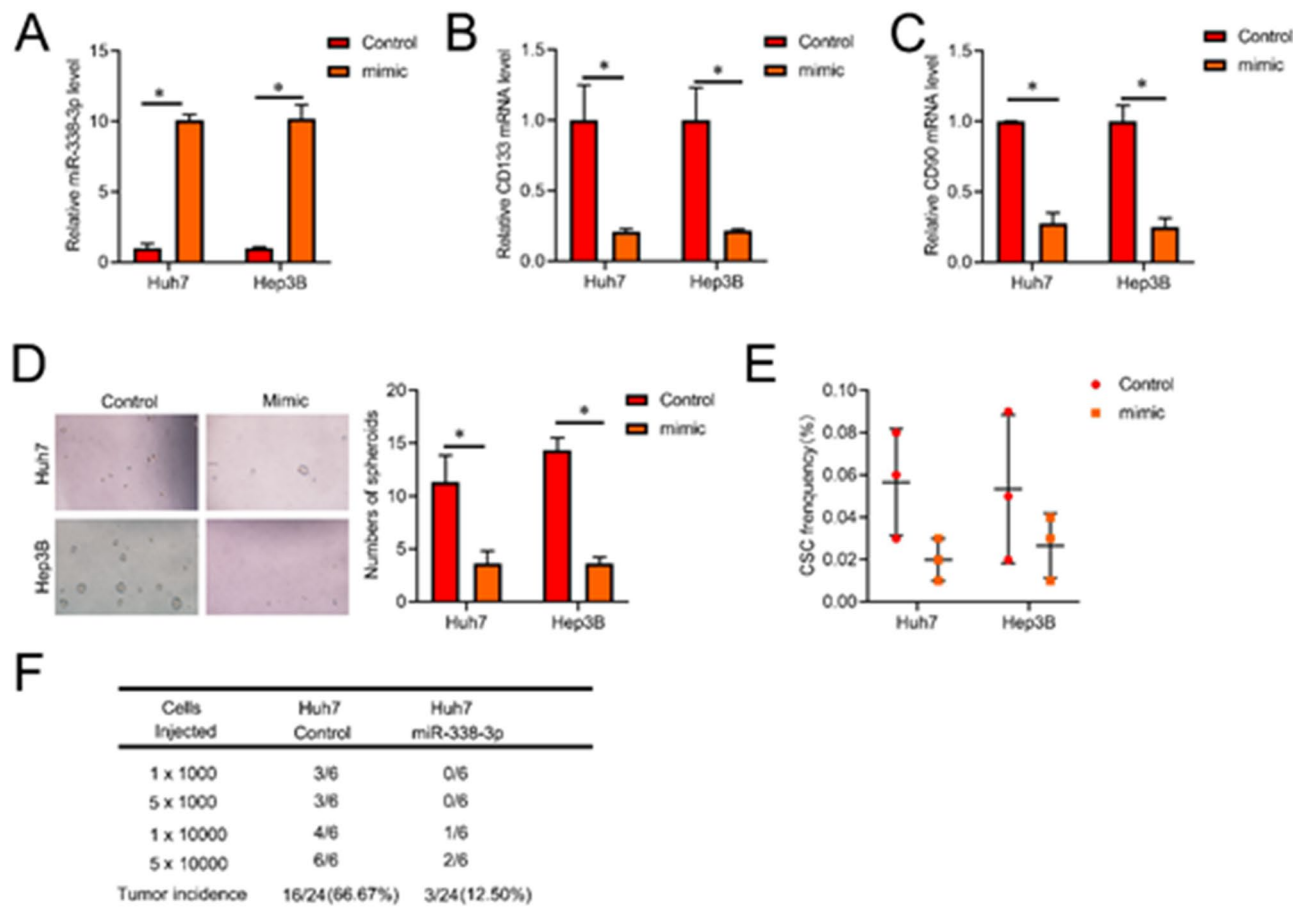


**Fig. 2.** miR-338-3p overexpression attenuates hepatic CSCs self-renewal and tumor development. (A) miR-338-3p overexpression virus was used to infect Huh7 and Hep3B cells, and their effects were then evaluated by RT-PCR. (B, C) Comparison of miR-338-3p overexpression cells and control HCC cells regarding CD133 and CD90 expression using RT-PCR. (D) Evaluation of miR-338-3p overexpressing cells and control HCC cells' ability to form spheroids. Representative images of spheres are shown. (E) In vitro LDA comparing the number of liver CSCs in cells with overexpressed miR-338-3p and control HCC cells. (F) miR-338-3p overexpressing cells and control HCC cells were subjected to an in vivo LDA. After eight weeks, tumors from each group ( $n=3$ ) were analyzed. Error bars shows mean  $\pm$  SD derived from  $n=3$  independent experiments,  $*p<0.05$ .

### Evaluation of lenvatinib response in HCC cells by miR-338-3p

There is growing evidence that CSCs have a role in controlling chemoresistance<sup>27</sup>. The levels of miR-338-3p were much lowered in Lenvatinib-resistant HCC cell lines, as shown in Fig. 5A. However, the introduction of SOX4 could reverse the sensitivity of miR-338-3p overexpressed HCC cells to cellular apoptosis induced by Lenvatinib (Fig. 5B). Furthermore, K-M evaluations were used to determine the survival time of HCC patients treated with Lenvatinib post-surgery. HCC individuals with elevated miR-338-3p expression showed a longer survival time following Lenvatinib therapy (Fig. 5C). The underlined findings implied that miR-338-3p could potentially predict a response to Lenvatinib.

### Discussion

Worldwide, HCC ranks as the 6th major cause of cancer-related fatalities. Recently many studies indicated miR-338-3p played key role in HCC, such as Huang, etc. had reported that miR-338-3p inhibited HCC epithelial-mesenchymal transition(EMT) and metastasis in HCC<sup>28</sup>. Beside, another study indicated that bone marrow mesenchymal stem cell-derived exosomal MiR-338-3p represses HCC progression by targeting ETS1<sup>29</sup>. Recently studies found that miR-338-3p was down-regulated by HBX and inhibits cell proliferation by targeting CyclinD1 and Foxp4 in HCC<sup>30,31</sup>. The probable function of miR-338-3p in hepatic CSCs is undetermined. In the present study, primary liver CSCs have been found to have reduced miR-338-3p expression levels. miR-338-3p plays an indispensable role in liver CSCs' self-renewal and tumor formation. Extensive mechanistic investigation of hepatic CSCs uncovered a previously unrecognized miR-338-3p/SOX4 regulatory mechanism. Overexpression of miR-338-3p reversed Lenvatinib resistance, highlighting its essential role in determining how HCC cells respond to treatment. The clinical benefit of Lenvatinib in HCC patients might be predicted by miR-338-3p based on the evaluations of a patient cohort.

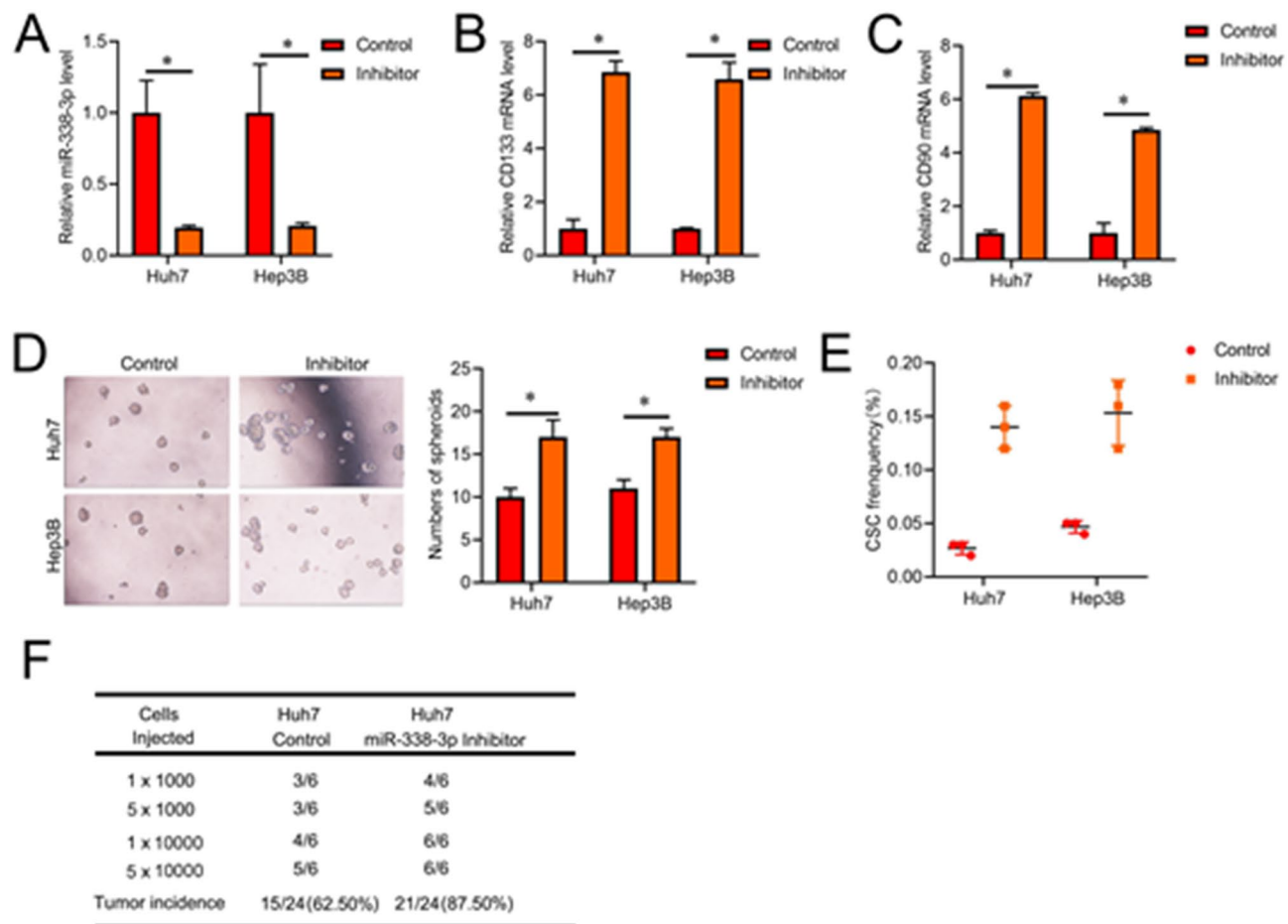


**Fig. 3.** miR-338-3p knockdown promotes liver CSCs self-renewal and tumor development. (A) RT-PCR experiment confirmed the infection of Huh7 and Hep3B cells with the miR-338-3p knockdown virus. (B, C) RT-PCR analysis of CD133 and CD90 expression in miR-338-3p-knockdown and control HCC cells. (D) MiR-338-3p knockdown and control HCC cells were tested for their ability to form spheroids. Representative images of spheres are shown. (E) Using an in vitro LDA, we evaluated the level of hepatic CSCs in cells with and without miR-338-3p. (F) miR-338-3p knockdown and control HCC cells were tested using an in vivo LDA. After 8 weeks, tumors from each group ( $n=6$ ) were analyzed. Error bars shows mean  $\pm$  SD derived from  $n=3$  independent experiments, \* $p<0.05$ ; NS  $p>0.05$ .

The importance of miRNAs for regulating CSCs or T-ICs has grown recently. Both loss and gain of miRNA contribute to CSCs self-renewal and tumorigenesis<sup>22–35</sup>. Specifically, miR-206 suppresses the growth of hepatic CSCs by reducing EGFR expression<sup>31</sup>, among other mechanisms of action. By controlling PTPN11 expression, miR-186 inhibits the growth of hepatic CSCs<sup>31,36</sup>. In OSCC, CD24 (a marker of CSCs) is regulated via the miR-146a/AKT/β-Catenin cascade<sup>37</sup>. Yet, miR-338-3p's probable function in hepatic CSCs is a mystery. The present findings indicate that miR-338-3p is suppressed in hepatic CSCs. Following the induced expression of miR-338-3p, transcriptional regulators of stemness and markers of CSCs were downregulated. CSCs can both start tumor growth and maintain themselves. Higher expression of miR-338-3p attenuated hepatic CSCs' self-renewal and tumor development, as indicated by our experiments. Our research showed the crucial part of miR-338-3p in developing liver CSCs and points to it as a potential target for treatment.

Herein, we identified the genes that miR-338-3p was targeting using bioinformatics. Additionally, we showed that SOX4 is one of the many possible genes we found that miR-338-3p might inhibit in liver CSCs. According to research, SOX4 is dysregulated in several cancerous tumor types<sup>38</sup>. In EMT, SOX4 has been shown to have a key role in recent research<sup>39</sup>. It was also revealed that SOX4 played a part in regulating CSCs<sup>34</sup>. Herein, it has been shown that miR-338-3p interacts with the 3'UTR of SOX4 in hepatic CSCs and reduces SOX4 expression. For the first time, SOX4 was assessed in our study as a direct target gene of miR-338-3p. Rescue tests confirmed that miR-338-3p attenuated the growth of hepatic CSCs by downregulating SOX4 expression. In fact, small RNAs play important biological roles and obviously not only target one gene. In previous studies, multiple important target genes of miR-338-3p have been mentioned, such as cyclinD1, FOXP4, and EST1<sup>29–31</sup>, etc. Therefore, we speculate that miR-338-3p attended to the growth of hepatic CSCs, which may not only through SOX4, and this is worthy of further research in the future.

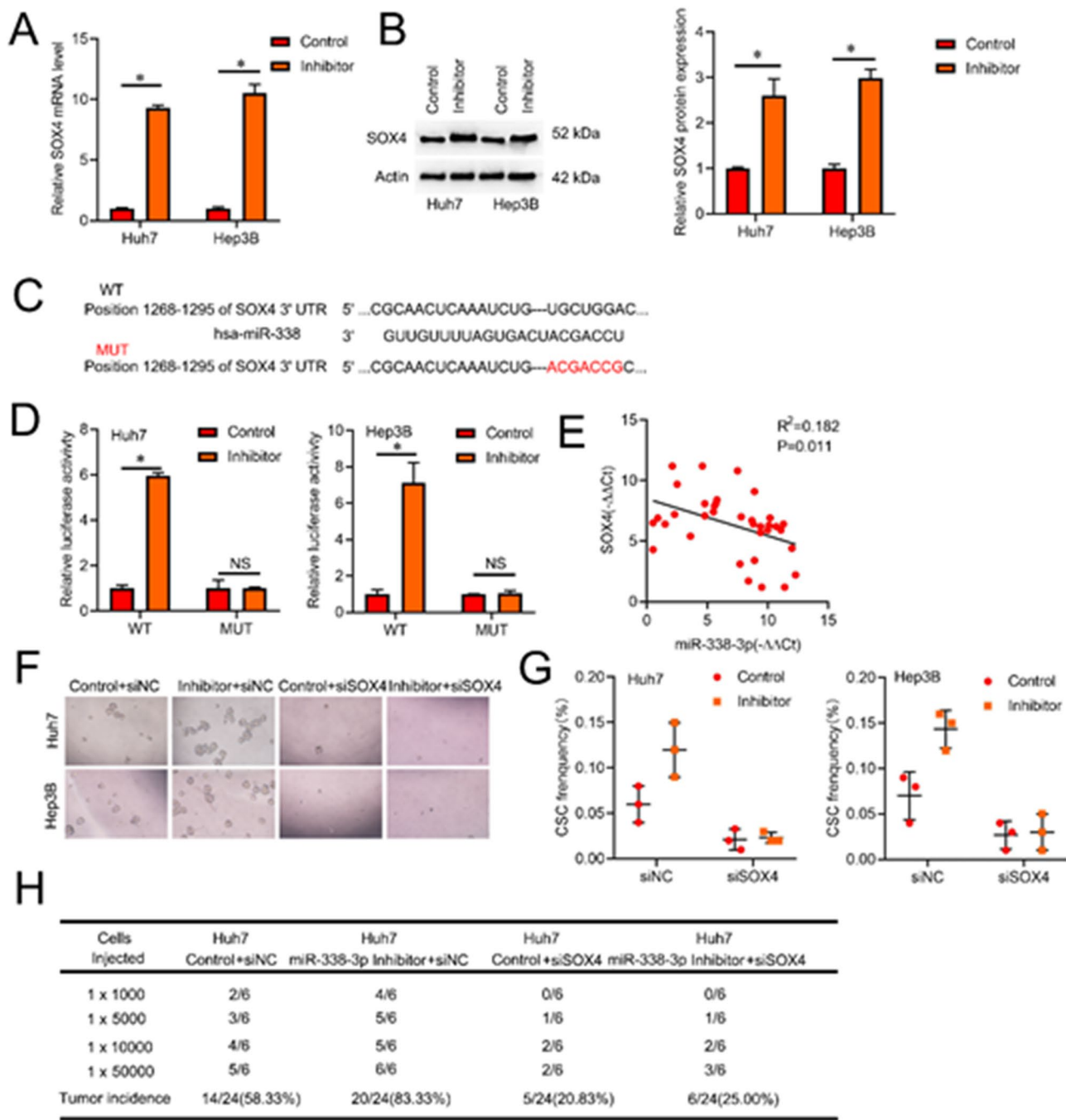


**Fig. 4.** miR-338-3p-mediated hepatic CSC self-renewal and tumor formation depend on SOX4. **(A)** Comparison of SOX4 expression in miR-338-3p knockdown against control HCC cells using RT-PCR. **(B)** left panel: SOX4 was examined by immunoblotting in miR-338-3p knockdown and untreated HCC cells. Right panel: quantification for SOX4 protein. **(C)** miR-338-3p binding sites in the 3'-UTR of the SOX4 gene and the nucleotides changed in the SOX4-3'UTR mutant were predicted using a Target Scan. **(D)** In control HCC cells and miR-338-3p knockdown cells, the luciferase activity of the SOX4-WT or SOX4-Mut 3'-UTR was assessed, and the relative activity was displayed. **(E)** Primary HCC cells ( $n=35$ ) were analyzed using RT-PCR for their miR-338-3p and SOX4 expression levels. Spearman's correlation analysis was performed after data were standardized to  $-\beta$ -actin as  $\Delta\Delta Ct$ . **(F)** HCC cells with and without miR-338-3p knockdown were transfected with SOX4 siRNA or negative control and then cultured to generate spheroids. **(G)** Transfection of SOX4 siRNA or negative control into miR-338-3p knockdown cells and control HCC cells was then exposed to an in vitro LDA. **(H)** To perform an in vivo LDA, HCC cells expressing miR-338-3p were transfected with SOX4 siRNA or an NC. Error bars shows mean  $\pm$  SD derived from  $n=3$  independent experiments,  $*p<0.05$ ; NS  $p>0.05$ .

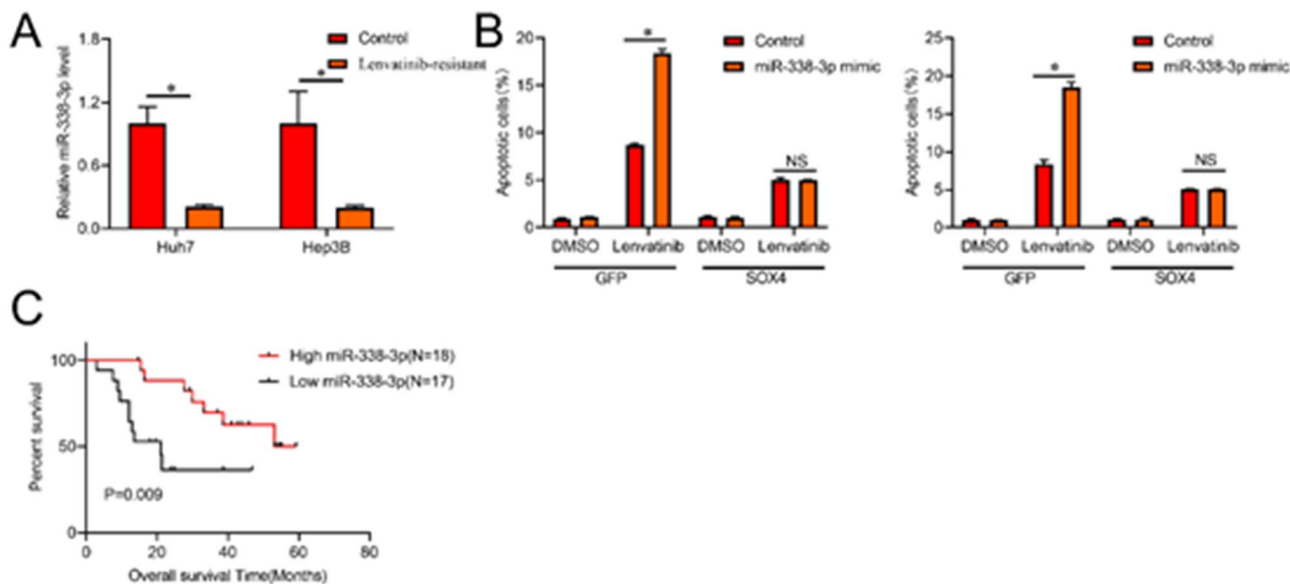


**Fig. 5.** miR-338-3p determines the response of Lenvatinib in HCC cells. (A) Comparison of Lenvatinib-resistant HCC cells and control HCC cells using RT-PCR. (B) miR-338-3p mimic and control HCC cells were infected with a negative control virus or overexpressing SOX4 and then treated with Lenvatinib (10  $\mu$ M) for 48 h. Flow cytometry was used to determine how many cells had undergone apoptosis. (C) K-M analysis was used to compare the overall survival of HCC patients in the miR-338-3p-high ( $n=18$ ) and miR-338-3p-low ( $n=17$ ) groups after treatment with Lenvatinib. Error bars shows mean  $\pm$  SD derived from  $n=3$  independent experiments,  $*p < 0.05$ ; NS  $p > 0.05$ .

First-line treatment of HCC with the oral multikinase inhibitor lenvatinib has been approved<sup>40,42</sup>. Lenvatinib is effective for many people with advanced HCC, yet, many patients quickly acquire resistance. Hence, it is critical to study the mechanisms behind Lenvatinib resistance and to establish accurate biomarkers of the drug's efficacy. The findings revealed that miR-338-3p overexpressing HCC cells are especially vulnerable to Lenvatinib's growth-inhibiting and apoptotic effects. Patients exhibiting elevated miR-338-3p expression had the longest post-treatment survival rates among individuals with HCC who had received lenvatinib after surgery, according to a K-M analysis of these patients. Therefore, to ascertain whether patients may benefit from Lenvatinib therapy, biomarker-guided clinical studies should determine the effectiveness of detecting the expression of miR-338-3p in HCC tumors.

## Conclusion

In conclusion, miR-338-3p has a considerable function in liver CSC self-renewal and tumor development, making it a promising therapeutic target against HCC. The paper still has shortcomings, such as lacking of miR-338-3p mimic delivery along with SOX4 and assess cancer incidence, and present the SOX4 levels in the in vivo experiments, worthing exploring in future research.

## Data availability

The data in the current study are available from the corresponding authors upon reasonable request.

Received: 26 March 2024; Accepted: 11 June 2025

Published online: 18 July 2025

## References

1. Siegel, R. L., Miller, K. D., Fuchs, H. E., Jemal, A. & Cancer Statistics CA Cancer J Clin 2021; 71:7–33. (2021).
2. Liu, X. et al. Higher whole grains and dietary fiber intake are associated with lower risk of liver cancer and chronic liver disease mortality. *Nat. Commun.* **12**, 6388 (2021).
3. Xiang, D. M. et al. Oncofetal HLF Transactivates c-Jun To Promote Hepatocellular Carcinoma Development and Sorafenib Resistance (Gut, 2019).
4. Jin, H. et al. EGFR activation limits the response of liver cancer to lenvatinib. *Nature* **595**, 730–734 (2021).
5. Huang, X. et al. Lenvatinib plus immune checkpoint inhibitors improve survival in advanced hepatocellular carcinoma: A retrospective study. *Front. Oncol.* **11**, 751159 (2021).
6. Rimini, M. et al. Nonalcoholic steatohepatitis in hepatocarcinoma: new insights about its prognostic role in patients treated with lenvatinib. *ESMO Open*. **6**, 100330 (2021).
7. Singh, A. K. et al. Tumor heterogeneity and cancer stem cell paradigm: updates in concept, controversies and clinical relevance. *Int. J. Cancer*. **136**, 1991–2000 (2015).
8. Kreso, A. & Dick, J. E. Evolution of the cancer stem cell model. *Cell. Stem Cell.* **14**, 275–291 (2014).
9. Liu, Y. et al. Comprehensive analysis of clinical significance of stem-cell related factors in renal cell cancer. *World J. Surg. Oncol.* **9**, 121 (2011).

10. Gao, Y. et al. Intratumoral stem-like CCR4 + regulatory T cells orchestrate the immunosuppressive microenvironment in HCC associated with hepatitis B. *J. Hepatol.* (2021).
11. Salvadori, G. et al. Fasting-mimicking diet blocks triple-negative breast cancer and cancer stem cell escape. *Cell. Metab.* **33**, 2247–2259e2246 (2021).
12. Lai, S. A. et al. Blocking Short-Form Ron eliminates breast Cancer metastases through accumulation of Stem-Like CD4(+) T cells that subvert immunosuppression. *Cancer Discov* (2021).
13. Bayik, D. & Lathia, J. D. Cancer stem cell-immune cell crosstalk in tumour progression. *Nat. Rev. Cancer.* **21**, 526–536 (2021).
14. Xiang, D. et al. Shp2 promotes liver cancer stem cell expansion by augmenting beta-catenin signaling and predicts chemotherapeutic response of patients. *Hepatology* **65**, 1566–1580 (2017).
15. Griesemer, D. et al. Genome-wide functional screen of 3'UTR variants uncovers causal variants for human disease and evolution. *Cell* **184**, 5247–5260e5219 (2021).
16. Magen, I. et al. Circulating miR-181 is a prognostic biomarker for amyotrophic lateral sclerosis. *Nat. Neurosci.* **24**, 1534–1541 (2021).
17. Mikami, Y. et al. MicroRNA-221 and – 222 modulate intestinal inflammatory Th17 cell response as negative feedback regulators downstream of interleukin-23. *Immunity* **54**, 514–525e516 (2021).
18. Winkle, M., El-Daly, S. M., Fabbri, M. & Calin, G. A. Non-coding RNA therapeutics - challenges and potential solutions. *Nat. Rev. Drug Discov.* **20**, 629–651 (2021).
19. Komoll, R. M. et al. MicroRNA-342-3p is a potent tumour suppressor in hepatocellular carcinoma. *J. Hepatol.* **74**, 122–134 (2021).
20. Yu, Z. et al. miRNA-338-3p inhibits glioma cell proliferation and progression by targeting MYT1L. *Brain Res. Bull.* **179**, 1–12 (2022).
21. Zhang, B., Wang, D., Wang, Y. & Chen, G. miRNA-338-3p inhibits the migration, invasion and proliferation of human lung adenocarcinoma cells by targeting MAP3K2. *Aging (Albany NY)* **14** (15), 6094–6110 (2022).
22. Mirzaei, S. et al. The role of microRNA-338-3p in cancer: growth, invasion, chemoresistance, and mediators. *Life Sci.* **268**, 119005 (2021).
23. Xiang, D. M. et al. Oncofetal HLF transactivates c-Jun to promote hepatocellular carcinoma development and Sorafenib resistance. *Gut* **68**, 1858–1871 (2019).
24. Yin, S. et al. CD133 positive hepatocellular carcinoma cells possess high capacity for tumorigenicity. *Int. J. Cancer.* **120**, 1444–1450 (2007).
25. Yang, Z. F. et al. Significance of CD90 + cancer stem cells in human liver cancer. *Cancer Cell.* **13**, 153–166 (2008).
26. Shen, H. et al. Sox4 expression confers bladder Cancer stem cell properties and predicts for poor patient outcome. *Int. J. Biol. Sci.* **11**, 1363–1375 (2015).
27. Yao, H. et al. miR-186 inhibits liver Cancer stem cells expansion via targeting PTPN11. *Front. Oncol.* **11**, 632976 (2021).
28. Chen, J. S. et al. miR-338-3p inhibits epithelial-mesenchymal transition and metastasis in hepatocellular carcinoma cells. *Oncotarget* **8** (42), 71418–71429 (2016).
29. Li, Y. H., Lv, M. F., Lu, M. S. & Bi, J. P. Bone marrow mesenchymal stem cell-derived Exosomal MiR-338-3p represses progression of hepatocellular carcinoma by targeting ETS1. *J. Biol. Regul. Homeost. Agents.* **35** (2), 617–627 (2021 Mar-Apr).
30. Fu, X., Tan, D., Hou, Z., Hu, Z. & Liu, G. miR-338-3p is down-regulated by hepatitis B virus X and inhibits cell proliferation by targeting the 3'-UTR region of CyclinD1. *Int. J. Mol. Sci.* **13** (7), 8514–8539 (2012). d.
31. Wang, G. et al. MicroRNA-338-3p inhibits cell proliferation in hepatocellular carcinoma by target forkhead box P4 (FOXP4). *Int. J. Clin. Exp. Pathol.* **8** (1), 337–344 (2015).
32. Khan, A. Q. et al. Role of miRNA-Regulated Cancer stem cells in the pathogenesis of human malignancies. *Cells* **8** (8), 840 (2019).
33. Venkatesh, J., Wasson, M. D., Brown, J. M., Fernando, W. & Marcato, P. LncRNA-miRNA axes in breast cancer: novel points of interaction for strategic attack. *Cancer Lett.* **509**, 81–88 (2021).
34. Li, L. et al. Epigenetic modification of MiR-429 promotes liver tumour-initiating cell properties by targeting Rb binding protein 4. *Gut* **64**, 156–167 (2015).
35. Han, T. et al. miR-552 regulates liver Tumor-Initiating cell expansion and Sorafenib resistance. *Mol. Ther. Nucleic Acids.* **19**, 1073–1085 (2020).
36. Liu, C. et al. miR-206 inhibits liver cancer stem cell expansion by regulating EGFR expression. *Cell. Cycle.* **19**, 1077–1088 (2020).
37. Ghuwalewala, S. et al. MiRNA-146a/AKT/beta-Catenin activation regulates Cancer stem cell phenotype in oral squamous cell carcinoma by targeting CD24. *Front. Oncol.* **11**, 651692 (2021).
38. Huang, J. L. et al. SOX4 as biomarker in hepatitis B virus-associated hepatocellular carcinoma. *J. Cancer.* **12**, 3486–3500 (2021).
39. Sandbothe, M. et al. The microRNA-449 family inhibits TGF-beta-mediated liver cancer cell migration by targeting SOX4. *J. Hepatol.* **66**, 1012–1021 (2017).
40. Gordan, J. D. et al. Systemic therapy for advanced hepatocellular carcinoma: ASCO guideline. *J. Clin. Oncol.* **38**, 4317–4345 (2020).
41. Han, T. et al. Downregulation of MUC15 by miR-183-5p.1 promotes liver tumor-initiating cells properties and tumorigenesis via regulating c-MET/PI3K/AKT/SOX2 axis. *Cell. Death Dis.* **13**, 200 (2022).
42. Wang, J. et al. N6-Methyladenosine-Mediated Up-Regulation of FZD10 Regulates Liver Cancer Stem Cells' Properties and Lenvatinib Resistance Through WNT/beta-Catenin and Hippo Signaling Pathways. *Gastroenterology.* (2023).

## Author contributions

All authors contributed to the study's conception and design. Study designs were performed by ZM L and LP Y. Material preparation and analysis were performed by ZM L and LP Y. Clinical data collection and analysis were performed by Y Y, HF L, ZM L and LP Y. Histological analyses were performed by Y Y, HF L, ZM L and LP Y. The manuscript was written and revised by Y Y, HF L, L O , ZM L and LP Y. All authors read and approved the final manuscript.

## Funding

This study was supported by the Scientific Research Project of Changning District Health[NO.20194Y001].

## Declarations

### Competing interests

The authors declare no competing interests.

### Ethics approval

The authors are accountable for all aspects of the work and for ensuring that questions related to the accuracy or integrity of any part of the work are appropriately investigated and resolved. The study was conducted in

accordance with the Declaration of Helsinki (as revised in 2013). The Ethics Committee of Tongren Hospital, Shanghai Jiao Tong University School of Medicine (Shanghai, China) approved this collection procedure and participants gave informed consent. All methods were carried out in accordance with relevant guidelines and regulations for human studies. Animal experiments were performed under a project license granted by ethics board of Second Military Medical University, in compliance with Tongren Hospital, Shanghai Jiao Tong University School guidelines for the care and use of animals. The maximal tumor size was less than 2000 mm<sup>3</sup> permitted by the Animal Care and Use ethics committee of the Tongren Hospital, Shanghai Jiao Tong University School of Medicine. The maximal tumor size in all mice involved in this study was not exceeded than 2000 mm<sup>3</sup>. The study was carried out in compliance with the ARRIVE guidelines.

### Additional information

**Supplementary Information** The online version contains supplementary material available at <https://doi.org/10.1038/s41598-025-06805-0>.

**Correspondence** and requests for materials should be addressed to H.-f.L., Z.-m.L. or L.-p.Y.

**Reprints and permissions information** is available at [www.nature.com/reprints](http://www.nature.com/reprints).

**Publisher's note** Springer Nature remains neutral with regard to jurisdictional claims in published maps and institutional affiliations.

**Open Access** This article is licensed under a Creative Commons Attribution-NonCommercial-NoDerivatives 4.0 International License, which permits any non-commercial use, sharing, distribution and reproduction in any medium or format, as long as you give appropriate credit to the original author(s) and the source, provide a link to the Creative Commons licence, and indicate if you modified the licensed material. You do not have permission under this licence to share adapted material derived from this article or parts of it. The images or other third party material in this article are included in the article's Creative Commons licence, unless indicated otherwise in a credit line to the material. If material is not included in the article's Creative Commons licence and your intended use is not permitted by statutory regulation or exceeds the permitted use, you will need to obtain permission directly from the copyright holder. To view a copy of this licence, visit <http://creativecommons.org/licenses/by-nc-nd/4.0/>.

© The Author(s) 2025